Effect of IR Radiation on Electrochemical Hydrogen Activity of Flexible Carbon-Palladium Dispersed Polymer Electrodes

R.N. Viswanath[iD]

Centre for Nanotechnology Research, Department of Humanities and Science, Aarupadai Veedu Institute of Technology, Vinayaka Mission's Research Foundation (DU), Paiyanoor, Chennai-603104, India

Corresponding author: E-mail: rnviswanath@avit.ac.in

Carbon-palladium dispersed polymer electrode sheets were synthesized and their hydrogen electrosorption (adsorption and absorption) and desorption activity on exposure to infra-red light radiation have been studied. Electrochemical experiments have been carried out in a standard glass electrochemical cell. The cyclic voltammograms of the carbon-palladium dispersed polymer electrode in 1 M NaCl electrolyte exhibit familiar features, namely hydrogen electrosorption and desorption peaks, adsorption of chlorine ions and a broad oxidative OH⁻ adsorption and desorption regions. The analysis of the cyclic voltammetry results suggests that the net charge transferred corresponding to the hydrogen electrosorption and desorption processes across the carbon-palladium electrode increases when exposed to infrared radiation. The analysis of the cyclic voltammetry results further suggested that the enhanced hydrogen activity across the flexible polymer supported carbon-palladium electrode surfaces with infrared light radiation is largely ascribed due to the removal of chlorine ions that are adsorbed partially over the surface of palladium clusters in the flexible carbon-palladium dispersed polymer supported flexible electrodes.

Keywords: Electrochemistry, Flexible electrodes, Hydrogen activity, Carbon-palladium dispersed polymer electrodes.

INTRODUCTION

Electrochemical devices for reversible hydrogen evolution reactions and double layer capacitive charging/discharging have attracted increasing interest and attention in several studies because of their potential in high power output and high energy density applications [1]. The mechanisms underlying to the reversible charge transfer electrochemical processes was reported at the early stages on planar single crystal noble metal electrodes [2-6]. It has only in the beginning of this century been explored that the electrochemical features of high energy storage capacity and catalytic hydrogen evolution process across the non-planar rough electrode surfaces. The relationship between the change in catalytic properties and specific capacitance (F/cm²) of such rough electrode materials has also been identified [7]. The rough surfaces are favourable for high ionic transports thus resulting in better charge transfer capability on compared to that of smooth planar surfaces. However, the cost of these pure planar and rough surface electrode materials is very high and restricted to use them for commercial electrochemical measurements and sensor devices.

The interest relevant to the development of such electrochemical devices comes in the context of developing high performance low cost carbon-metal based hierarchical structured electrodes [8]. Metal coated per-fluorinated polymer membrane and carbon-polymer composite are the exemplary modified electrode materials developed for this purpose [9]. Despite the number of reports, modified electrodes made by the combination of metals and carbon associated with polymeric species produce encouraging results. The carbon-metal electrodes dispersed in the polymeric medium yielded a number of interesting features like highly flexible, low cost, easy to handle and can be shaped in to different device geometry. Additional advantage of using polymer supported carbon-metal electrodes is their porous morphology and momentous technological importance, for instance, in relation to light weight with high power delivery [10]. Porous materials with hierarchical structures proposed for hydrogen evolution reactions are advantageous: electrolyte can impregnate quickly through the interconnected free-spaces by means of weak capillary forces and interact with active atom sites in pore surface regions [11-13]. For instance, estimating the diffusion distance at √Dt, time required for diffu-

sing hydrogen from the surface to the centre of a 10 nm particle is obtained as 3 μs, suggesting that almost instantaneous equilibrium of hydrogen in nanoparticles has been achieved in a short period [14].

Significant efforts have been made for the development of flexible porous hierarchical electrodes by combining materials of different functional characters in order to meet new engineering challenges and innovate their development capabilities for various applications [15-17]. Most of such electrodes are in complex form and have the capability of making eco-friendly products for sensing, energy storage and energy conversion applications [18-20]. In line with recent advances in electric energy powered electrochemical devices, the storage of electrical energy through hydrogen evolution reactions have become promising in diverse fields. The working performance of such hydrogen energy storage devices can be achieved for normal operations by means of creating (i) excellent recyclability with cyclic lives of hundreds of thousands of cycles, (ii) substantially greater power density and (iii) reproducible state of charge indication during charging/discharging. In view of the practical requirement for the successful development of electrochemical systems, flexible polymer electrodes is considered as promising materials for state-off-the-art electrochemical electrodes owing to their high surface area, high power density, fast energy storage activity and ultra-long cycle life.

Fabrication of carbon-metal dispersed polymer electrodes and study of their microstructure dependent capacitive energy storage density and hydrogen evolution activity is relatively a new research topic. The challenges in the fabrication of such electrochemical devices with enhanced capacitive with high sensitive hydrogen evolution activity lay mainly on the mechanical stability of the flexible electrodes and their excellent energy storage properties [21,22]. In view of the practical requirement for the successful development of electrochemical systems, carbon-metal dispersed polymer electrodes are considered as promising materials for state-off-the-art electrochemical electrodes owing to their high surface area, high power density, fast energy storage activity and ultra-long cycle life.

The primary goal of the work described in this article is to produce large scale polymer supported carbon-metal hierarchical sheet electrodes with optimal properties for applications, aiming specifically at extremely large surface area and thermal stability. The article also discusses the importance of the study, connecting the electrochemistry on porous solid surfaces to the superfunctional electrochemical capacitors with the stable catalytic properties for advanced technology. In this study, flexible carbon-palladium dispersed polymer sheets of different dimensions have been prepared and their hydrogen electro-sorption/desorption behaviour prior to and after exposure to infrared light radiation have been studied. The uniqueness to the development of flexible carbon-palladium dispersed polymer comes in the context of designing high performance electrodes having reduced concentration of precise metals [23,24].

EXPERIMENTAL

The procedure involved in the synthesis of flexible carbon-palladium dispersed polymer electrodes is briefly described below. Carbon in powder form has been produced from an incomplete combustion reaction [25]. Ultra-fine Palladium powder of mean diameter 8 ± 2 nm was procured from Sigma Aldrich®. Commercial Grade toxic free FEVI Gun (Brand: Pidilite) was used as a synthetic adhesive polymer. Homogeneous mixing of carbon, ultra-fine Pd powders in to synthetic adhesive polymer is the most important process step involved in the preparation of the flexible C-Pd electrodes. At the beginning, ultra-fine Pd powders (5 wt.%) and carbon powders (95 wt.%) were ground using a laboratory mixer. Subsequently, the C-Pd mixture was dispersed uniformly into the pre-polymer synthetic adhesive in 1:2 volume ratios at 298 K. Then, the C-Pd dispersed pre-polymer was poured into Teflon templates of depth 2 mm for 2 h and kept in aqueous solution of 1 M NaCl for 10-12 h at 298 K. The resulting 2 mm thick sheets obtained were rinsed with ultra-pure 18.2 MΩ-cm water and used for further studies.

Since, the microstructure of the C-Pd dispersed polymer electrodes could have an impact on electrochemical hydrogen absorption/desorption properties, a piece cut from the prepared C-Pd dispersed polymer sheet was dried in N_2 stream and investigated in a Carl-Zeiss Supra 55 scanning electron microscope (SEM). Raman spectroscopy and photoluminescence measurements were carried out on the cut piece using an advanced micro-Raman spectrometer (Renishaw in Via) with an excitation light source of wavelength 532 nm using solid state laser with a power of 0.02 mW. The CCD detector attached to the instrument collects the Raman scattered and luminescence signals from the backscattering geometry with a laser spot size of 0.7 μm. A commercial potentiostat (PGSTAT 302N, Metrohm Autolab e.v.) was used to carry out the electrochemical experiments. All the electrochemical measurements were performed in 1 M NaCl electrolyte in a glass three electrode cell under potential control using Ag/AgCl/3 M KCl reference electrode. Two sheets of dimension 1 cm × 1 cm cut from a prepared C-Pd dispersed polymer sheet served as working and counter electrodes. The electrochemical experiments were carried out in a dark room to avoid the influence of any visible light induced charge-transfer reactions across the electrochemical interface. The potentiostat's current integration mode was enabled during the cyclic current (I) *versus* potential (E) scan to determine accurately the net-charge transferred to (or from) the working electrode. Prior to the electrochemical experiments, the glass cell was cleaned with concentrated nitric acid and rinse repeatedly with ultra-pure water (18.2 MΩ) to remove the adsorbed organic impurities at the surface of inner cell wall.

RESULTS AND DISCUSSION

Fig. 1a-b shows the typical photograph of C-Pd dispersed polymer sheet electrodes. As illustrated in Fig. 1c, the C-Pd dispersed polymer electrodes are flexible and easy to bend [26]. The schematic structure of C-Pd dispersed polymer is shown in Fig. 1d.

A few selected SEM micrograph images of the carbon-palladium dispersed polymer electrodes are depicted in Fig. 2. Fig. 2a illustrates surface-view SEM micrograph of a carbon-palladium dispersed polymer electrode. A continuous fibrous skin-like structure has been observed. The cross-section SEM
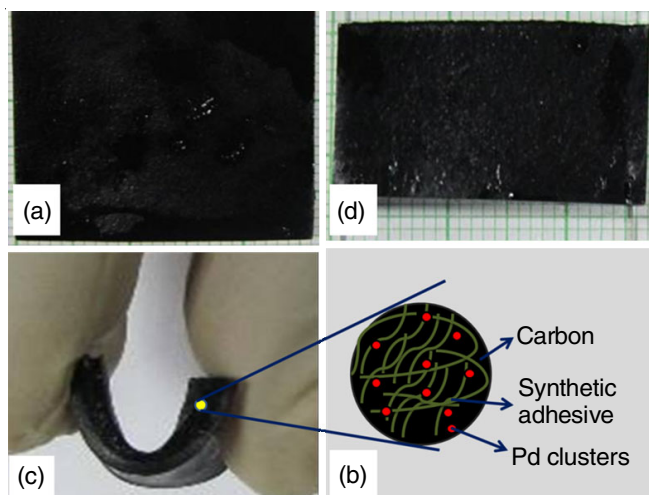
Fig. 1.   Photograph of flexible C-Pd dispersed polymer electrodes. (a), (b) as-prepared C-Pd dispersed polymer electrodes (front view). (c) Photograph of a mechanically bend C-Pd dispersed polymer sheet. (d) Schematic structure of the prepared carbon-palladium dispersed polymer
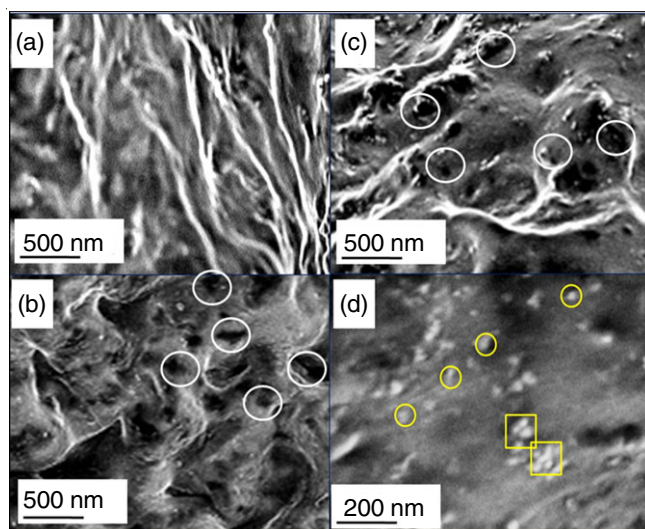

Fig. 2.   Representative surface and cross section views SEM images of carbon-palladium dispersed polymer sheet electrode. (a) Surface view. (b), (c) Cross section views. An assembly of skinny-layer with random porous morphology are seen in the micrographs. (d) Palladium ultra-fine particles dispersed in the form of isolated clusters (identified by yellow circles) and aggregates (identified by yellow squares)

micrographs of carbon-palladium dispersed polymer electrodes taken in two locations are as shown in Figs. 2b-c. It is seen that these micrographs are very close to the reported SEM micrograph of carbon dispersed polymer system [27]. The analysis of the SEM micrographs reveals that the overall microstructure of the carbon-palladium dispersed polymer electrodes is an assembly of continuous fibrous skinny layers. Interestingly, uneven spherical shaped image contrast, representative of pores, is found in a number of places in the SEM micrographs. A few of them are identified by white circle in Figs. 2b-c. On a closer observation of SEM micrograph of Fig. 2d, it has been revealed that majority of dispersed Pd particles in the polymer-carbon layers are in the form of isolated clusters (yellow circles), however, some clusters exist as aggregates (yellow squares).

Fig. 3a shows typical Raman spectrum of the C-Pd dispersed polymer electrode. It is seen that there are two Raman scattering bands D and G centred at 1367 and 1588 cm^{-1}, respectively present in the spectrum. The appearance of these two peak profile is qualitatively similar to that reported on Pd containing carbon films [28,29]. The analysis of the Raman spectrum reveals that the G band corresponds to the vibration of SP^2 bonded carbon atoms [30] and the D band is linked to lattice defects or structural disorder [31,32]. Fig. 3b shows its photoluminescence spectrum and it gives four luminescence peaks with their peak maximum at 560, 590, 630 and 700 nm, respectively. Lee *et al.* [33] and
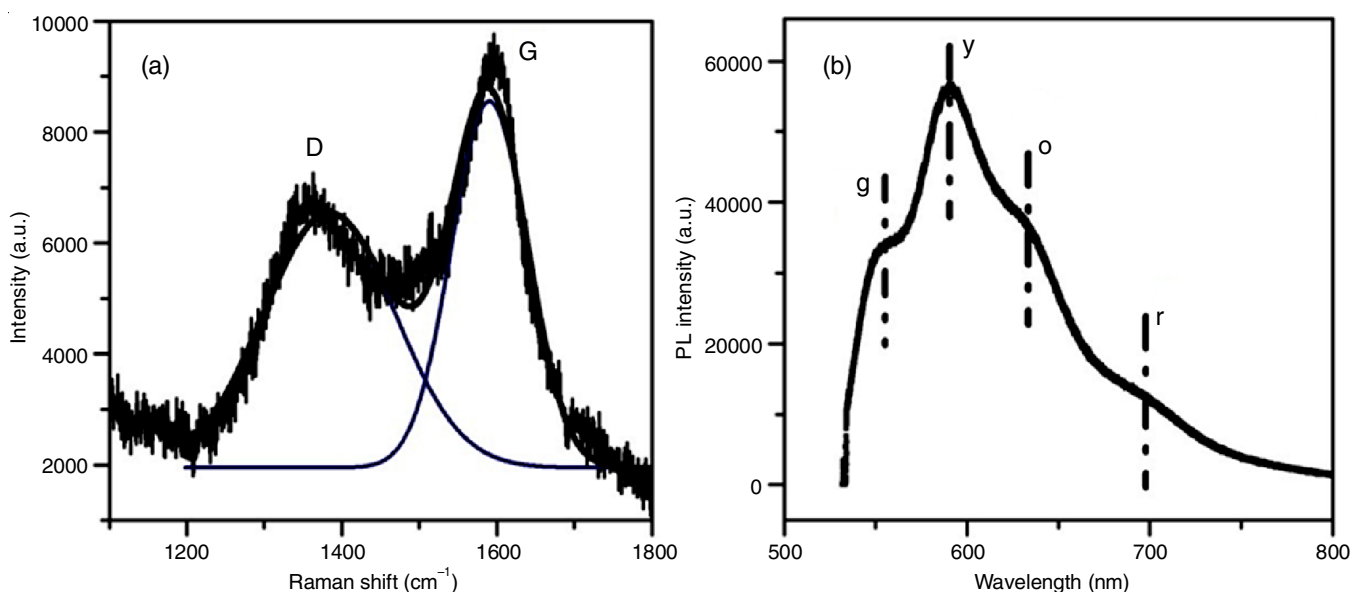

Fig. 3.   Raman and photoluminescence results of C-Pd dispersed polymer. (a) Raman spectrum of flexible C-Pd dispersed polymer showing Raman scattering peaks, characteristic of graphitic structures (D peak: 1360 cm^{-1}) and amorphous carbon (G peak: 1590 cm^{-1}). (b) Photoluminescence spectrum of flexible C-Pd dispersed polymer electrode, showing four luminescence peaks

Wang *et al.* [34] demonstrated from their photoluminescence studies that carbon particles emit visible radiation. This suggests that the emission peaks appeared in the photoluminescence spectrum of Fig. 3b corresponds to carbon quantum structures.

Although many uses have been proposed for the flexible sheet electrodes, we explored the infrared light radiation induced hydrogen sorption activity in 1 M NaCl electrolyte. Fig. 4a displays two successive cyclic voltammograms (CVs) for a C-Pd dispersed polymer electrode recorded in a wider potential interval, $-0.9 < E < 0.56$ V, at a scan rate of 10 mV s^{-1}. The arrows in the figure indicate the potential region in which the hydrogen sorption/desorption processes dominantly present. A strong hysteresis in these sorption/desorption processes was observed. This may be due to the potential gradient in the hierarchically structured C-Pd dispersed polymer membrane electrodes arising from the electrical resistance of the neutral 1 M NaCl electrolyte. Earlier reported results on porous Pd and porous Pt electrodes in a nearly neutral NaF electrolyte have also shown similar hysteretic behaviour in the hydrogen sorption/desorption reactions [35,36].

Besides the hydrogen sorption/desorption features as mentioned above, intense and sharp peaks appear in the anodic and cathodic scans in the potential interval, $0.1 < E < 0.3$ V, where the electro-sorption of hydrogen and oxygen containing ads-species are found to be absent. Since the origin of these sharp peaks appeared in the potential interval, $0.1 < E < 0.3$ V is not well understood, we carefully examined their stability. Fig. 4b shows the cyclic voltammetry scans of a C-Pd dispersed polymer electrode recorded in the narrow potential interval, $0.1 < E < 0.3$ V. It is observed that the current I value decreases from scan to scan and reach to almost a constant current value in both anodic and cathodic scans.

Understanding the surface sensitivity of polymer supported electrodes containing of electrochemical active nano-particulates

is important, because by deteriorating the secondary adsorbed species over the active surface of nano-particulates, if any present, their effective hydrogen activity can be studied. For instance, Arenz *et al.* [37] investigated the effect of chloride adsorption on the electrochemical behaviour of Pd ultra-thin film deposited on Pt (111) surface. Their results point out that chlorine anions strongly interact with Pd surface atoms and limit the sorption of hydrogen ad-atoms. Based on this established facts and the other literature reports, it is inferred that the reduction in the amplitude of current value in the voltage sweep in the potential interval, $0.1 < E < 0.3$ V (Fig. 4b) is mainly due to the presence of chlorine ad-layer around the Pd surfaces in the C-Pd dispersed polymer electrode.

As indicated earlier, the present study aims at determining the hydrogen sorption/desorption behaviour of C-Pd dispersed polymer electrodes on exposure to infrared light radiation. Viswanath & Weissmueller [14] in one of their earlier reports on electro-capillary coupling coefficients of hydrogen electro-sorption on Pd, pointed out that hydrogen transport in nanometer scaled Pd particles is quite faster and reached instantaneous equilibrium of hydrogen between the Pd surface and Pd core in less than 3 µs [38].

In order to investigate precisely the hydrogen sorption/desorption activity in C-Pd dispersed polymer electrodes, we imposed cyclic voltammograms in selected potential interval $-0.8 < E < 0.3$ V, where the hydrogen electro-sorption dominate. Fig. 5 displays the typical cyclic voltammogram of C-Pd dispersed polymer electrode recorded in the interval, $-0.8 < E < 0.3$ V, at a scan rate of 10 mV s^{-1}.

Now, let us discuss the results obtained from the hydrogen sorption/desorption reactions in the presence of infrared light radiation. The net charge transferred that corresponds to complete desorption or adsorption of hydrogen (ΔQ_H) using the relation is determined:
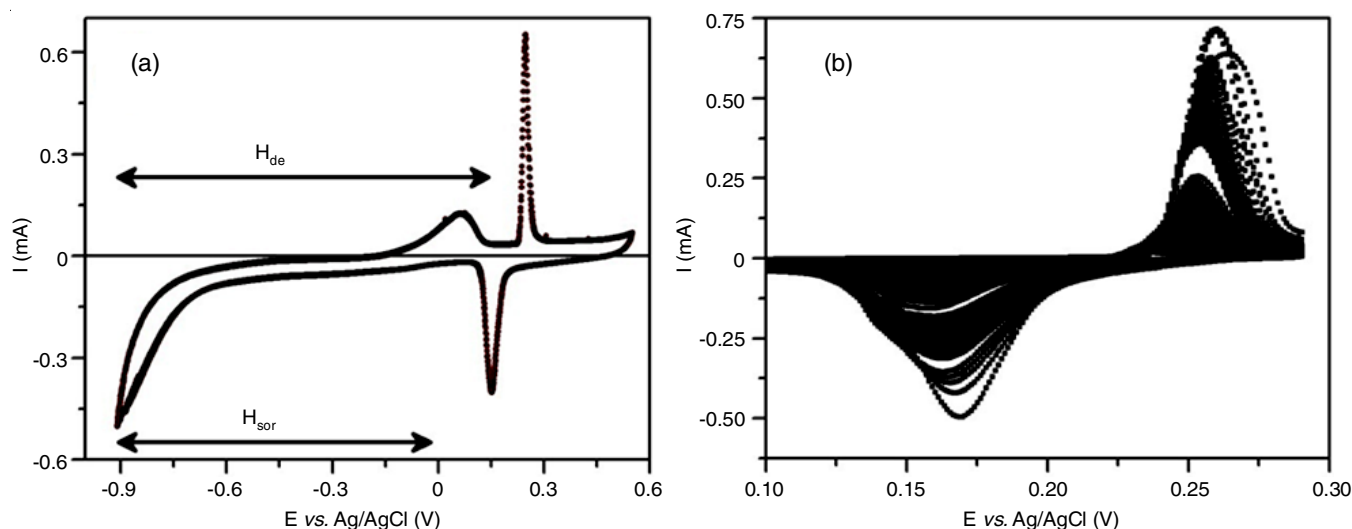

Fig. 4. Cyclic voltammetry results of C-Pd dispersed polymer electrode. (a) Cyclic voltammograms of C-Pd dispersed polymer electrode in 1 M NaCl electrolyte in the potential interval, $-0.9 < E < 056$ V *versus* Ag/AgCl. The potential intervals corresponding to the dominant hydrogen sorption/desorption and OH$^-$ adsorption/desorption processes are indicated by arrows. (b) Two hundred and thirty successive cyclic voltammograms recorded in the potential interval, $0.1 < E < 0.3$ V, where hydrogen and oxygen sorption/desorption reactions are found to be absent. Note that the current I value in sub figure b decreases from scan to scan and reach to almost a constant current passed region
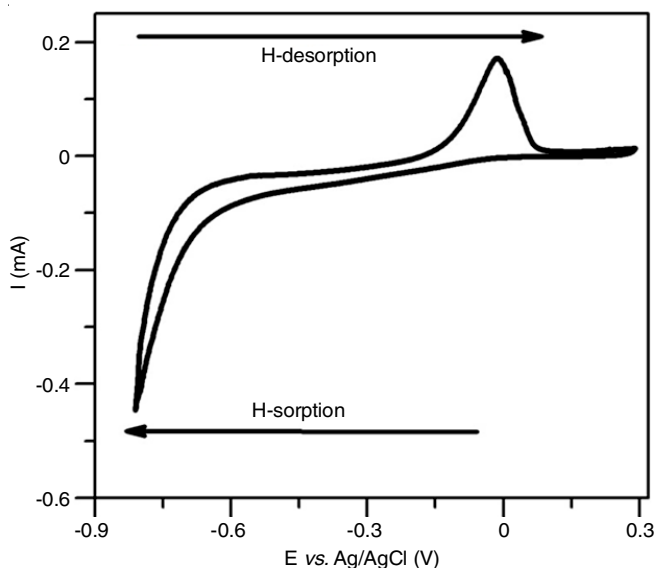
Fig. 5.   Typical cyclic voltammetry spectrum of flexible polymer supported carbon-palladium electrode in 1 M NaCl electrode recorded in the hydrogen sorption/desorption dominating potential intervals, -0.8 < E < 0.3 V at a scan rate of 10 mV/s

$$\Delta Q_H = \frac{1}{\nu} \int_{t_i}^{t_f} IdV$$

where I is the current passed with a linear sweeping voltage dV at a scan rate ν of 10 mV/s [39].

Top panel in Fig. 6 displays the potential *versus* time plot for the cyclic voltammetry during the anodic and cathodic potential sweep and the bottom panel illustrates the time dependent variation of charge ΔQ_H with electrode potential in the hydrogen electrosorption dominating potential interval, -0.8 < E < 0.3 V. It is observed that the amplitude of charge ΔQ_H remains constant up to ten cycles, increases gradually from 11 to 25 scans and decreases further with the increase of cyclic scan numbers from 26 to 50. It is worth to note that among the 50 scans ΔQ_H *versus* time curves obtained from the successive
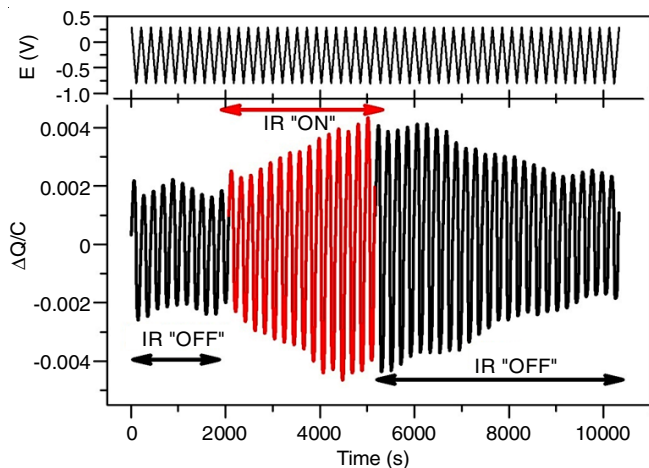

Fig. 6.   Potential E and variation of hydrogen charge ΔQ_H transferred across flexible C-Pd dispersed electrode during fifty successive cyclic scan in the potential interval -0.8 < E < 0.3 V. The measurement scan rate was 10 mV/s. It is noting that the infrared light turns "ON" during the cyclic scans from 11 to 25

cyclic current-potential scans, the infra red light source turns "OFF" except the cyclic scans from 11 to 25. The constant ΔQ_H value obtained from the cyclic scans 1-10 suggests that hydrogen charge transfer reaction occurring in C-Pd dispersed polymer electrode is found to be stable in spite of repeated cyclic scans. Importantly, the amplitude of the charge ΔQ_H value increases in the cyclic scans 11-25, where the infrared light source turns "ON".

Since, the enhancement of hydrogen activity in C-Pd dispersed polymer electrodes with IR radiation is an outstanding problem in catalysis science, we follow an analytical approach to unravel its origin. On a closer look of the voltammetry scans recorded in the potential interval -0.8 < E < 0.3 V, it is found that along with an increase of the current value, the hydrogen desorption peak shifts towards negative anodic potentials with infrared radiation. Fig. 7 shows the potential shift of hydrogen desorption peak E_P with voltammetry scan number N. The symbols o and □ identify the E_P value obtained from the voltammograms when the infrared source turns "ON" (scan nos. from 11 to 25) and "OFF" (scan nos. 26 to 40), respectively. A reversible shift in the potential value of -58 mV was observed. At the first approximation, the author assumed that the potential shift -58 mV observed can be attributed to any one of the three reasons *viz*., heating due to infrared excitation, variation of electrolyte pH and adsorption of anions [40-42].
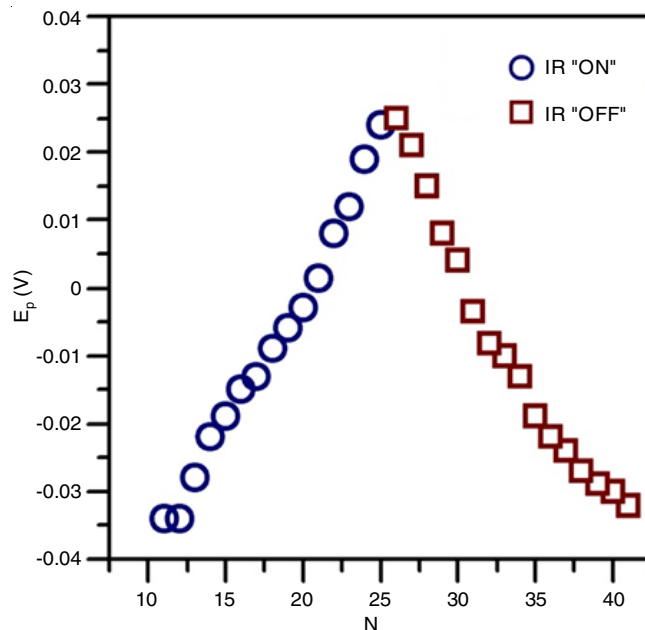

Fig. 7.   Hydrogen desorption peak potential E_P value with scan number N. The symbols o and □ identify the shift in the hydrogen desorption potential E_P value obtained from the voltammograms when the infrared source turns "ON" (scan nos. from 11 to 25) and "OFF" (scan nos. 26 to 40), respectively

Zalineeva *et al*. [43] through their electrochemical cyclic voltammetry studies in the temperature range of 296 ≤ T ≤ 333 K in an aqueous electrolyte confirmed that the amount of hydrogen electrosorption and desorption in palladium nanoparticles is not affected by the measurement temperature. Further, as the hydrogen ion activity relates to the pH value

with electrode potential according to the Nernst equation [44], it becomes necessary to verify the variation of pH value to the potential shift of the hydrogen desorption current peak in the voltammetry curves (Fig. 7). But, it is a known fact that neutral or nearly neutral electrolytes such as 1 M NaCl used in the present study do not affect their pH value. Therefore, having ruled out the possibilities of the role of temperature or pH value to the driving force for the shift of hydrogen desorption peak profiles, we are led to examine the effect of anion coverage around the hydrogen active Pd sites to the potential shift of hydrogen desorption current peak in the voltammetry curves (Fig. 7).

It must be mentioned that the voltammetry results depicted in Fig. 4a are obtained on the C-Pd dispersed polymer electrode prior to the cycling in the potential intervals $0.1 < E < 0.3$ V where chlorine anions mask the Pd catalytic sites. These results lead us to speculate that the retention of chlorine anions surrounding the Pd clusters in the C-Pd dispersion polymer electrode is responsible for the observed increase in hydrogen activity under infrared light radiation. This is further confirmed from nearly the same cumulative excess charge 20 mC estimated from successtive cyclic voltammery scans corresponding to the infrared light source and the cumulative charge estimated from the successive cyclic voltammetry scans (Fig. 4b) corresponding to the chlorine adsorption.

Conclusion

In summary, a flexible C-Pd dispersed polymer electrode is successfully synthesized in various dimensions using materials processing strategy of homogenization and condensation procedures at room temperature. The hydrogen electrosorption and desorption results obtained on C-Pd dispersed polymer electrode in 1 M NaCl electrolyte in infrared light turns "ON" and "OFF" conditions are quite interesting. A significant enhancement in the hydrogen sorption and desorption activities has been observed when exposed the electrolyte impregnated flexible in 1 M NaCl electrolyte to infrared light radiation. In addition to the enhancement of hydrogen charge transfer activities in C-Pd dispersed polymer electrode with infrared light radiation, the hydrogen desorption peak potential shifted towards more negative anodic potentials. This suggests that the dissolution of chlorine anions around the Pd active sites in the presence of infrared light radiation can be linked directly to the rearrangements of surface Pd atoms in C-Pd dispersed polymer electrode. The present study suggests that the C-Pd dispersed polymer electrodes can expand the possibility of developing commercial grade flexible lightweight electrodes for power sources and biomedical industries operating at the low electric potentials.

REFERENCES

1. C.G. Zoski, Handbook of Electrochemistry, Elsevier Science: New York, USA, edn. 1 (2007).
2. P. Simon and Y. Gogotsi, *Nat. Mater.*, **7**, 845 (2008);
   https://doi.org/10.1038/nmat2297
3. B.E. Conway, Electrochemical Supercapacitors, Kluwer Academic/ Plenum Publishers: New York (1999);
   https://doi.org/10.1007/978-1-4757-3058-6
4. R. Chattot, I. Martens, M. Mirolo, M. Ronovsky, F. Russello, H. Isern, G. Braesch, E. Hornberger, P. Strasser, E. Sibert, M. Chatenet, V. Honkimäki and J. Drnec, *J. Am. Chem. Soc.*, **143**, 17068 (2021);
   https://doi.org/10.1021/jacs.1c06780
5. H. Angerstein-Kozlowska, B.E. Conway, A. Hamelin and L. Stoicoviciu, *J. Electroanal. Chem. Interfacial Electrochem.*, **228**, 429 (1987);
   https://doi.org/10.1016/0022-0728(87)80122-5
6. B.E. Conway, *Prog. Surf. Sci.*, **49**, 331 (1995);
   https://doi.org/10.1016/0079-6816(95)00040-6
7. P. Simon and Y. Gogotsi, *Philos. Trans. Royal Soc. Math. Phys. Eng. Sci.*, **368**, 3457 (2010);
   https://doi.org/10.1098/rsta.2010.0109
8. H. Kang, S. Jung, S. Jeong, G. Kim and K. Lee, *Nature Commun.*, **6**, 6503 (2015);
   https://doi.org/10.1038/ncomms7503
9. I. Rubinstein and A.J. Bard, *J. Am. Chem. Soc.*, **102**, 6641 (1980);
   https://doi.org/10.1021/ja00541a080
10. F.L.M. Sam, G.D.M.R. Dabera, K.T. Lai, C.A. Mills, L.J. Rozanski and S.R.P. Silva, *Nanotechnology*, **25**, 345202 (2014);
    https://doi.org/10.1088/0957-4484/25/34/345202
11. R.F. Lane and A.T. Hubbard, *J. Phys. Chem.*, **77**, 1401 (1973);
    https://doi.org/10.1021/j100630a018
12. J. Weissmüller, R.N. Viswanath, D. Kramer, P. Zimmer, R. Würschum and H. Gleiter, *Science*, **300**, 312 (2003);
    https://doi.org/10.1126/science.1081024
13. D. Kramer, R.N. Viswanath and J. Weissmüller, *Nano Lett.*, **4**, 793 (2004);
    https://doi.org/10.1021/nl049927d
14. R.N. Viswanath and J. Weissmüller, *Acta Mater.*, **61**, 6301 (2013);
    https://doi.org/10.1016/j.actamat.2013.07.013
15. L.L. Miller and M.R. Van de Mark, *J. Electroanal. Chem. Interfacial Electrochem.*, **88**, 437 (1978);
    https://doi.org/10.1016/S0022-0728(78)80133-8
16. I. Streeter, R. Baron and R.G. Compton, *J. Phys. Chem. C*, **111**, 17008 (2007);
    https://doi.org/10.1021/jp076923z
17. M. Shahinpoor and K.J. Kim, *Smart Mater. Struct.*, **10**, 819 (2001);
    https://doi.org/10.1088/0964-1726/10/4/327
18. Yu.N. Gartstein, A.A. Zakhidov and R.H. Baughman, *Phys. Rev. B Condens. Matter*, **68**, 115415 (2003);
    https://doi.org/10.1103/PhysRevB.68.115415
19. C. Bianchini and P.K. Shen, *Chem. Rev.*, **109**, 4183 (2009);
    https://doi.org/10.1021/cr9000995
20. A.T. Haug, R.E. White, J.W. Weidner, W. Huang, S. Shi, T. Stoner, N. Rana and *J. Electrochem. Soc.*, **149**, A280 (2002);
    https://doi.org/10.1149/1.1446082
21. S.H. Lee, R.A. DeMayo, K.J. Takeuchi, E.S. Takeuchi and A.C. Marschilok, *J. Electrochem. Soc.*, **162**, A69 (2015);
    https://doi.org/10.1149/2.0351501jes
22. F.L.M. Sam, G.D.M.R. Dabera, K.T. Lai, C.A. Mills, L.J. Rozanski and S.R.P. Silva, *Nanotechnology*, **25**, 345202 (2014);
    https://doi.org/10.1088/0957-4484/25/34/345202
23. A.T. Haug, R.E. White, J.W. Weidner, W. Huang, S. Shi, T. Stoner and N. Rana, *J. Electrochem. Soc.*, **149**, A280 (2002);
    https://doi.org/10.1149/1.1446082
24. E. Antolini, S.C. Zignani, S.F. Santos and E.R. Gonzalez, *Electrochim. Acta*, **56**, 2299 (2011);
    https://doi.org/10.1016/j.electacta.2010.11.101

25. D. Mohapatra, S. Badrayyana and S. Parida, *Mater. Chem. Phys.*, **174**, 112 (2016);
https://doi.org/10.1016/j.matchemphys.2016.02.057

26. L. Bokobza, *Polymer*, **48**, 4907 (2007);
https://doi.org/10.1016/j.polymer.2007.06.046

27. C.Z. Chen, *Prog. Nat. Sci.*, **23**, 245 (2013);
https://doi.org/10.1016/j.pnsc.2013.04.001

28. X. Yan, T. Xu, S. Xu, X. Wang and S. Yang, *Nanotechnology*, **15**, 1759 (2004);
https://doi.org/10.1088/0957-4484/15/12/011

29. M. Zeiger, N. Jäckel, V.N. Mochalin and V. Presser, *J. Mater. Chem. A Mater. Energy Sustain.*, **4**, 3172 (2016);
https://doi.org/10.1039/C5TA08295A

30. F. Tuinstra and J.L. Koenig, *J. Chem. Phys.*, **53**, 1126 (1970);
https://doi.org/10.1063/1.1674108

31. X. Yan, T. Xu, S. Xu, X. Wang and S. Yang, *Nanotechnology*, **15**, 1759 (2004);
https://doi.org/10.1088/0957-4484/15/12/011

32. M. Zeiger, N. Jäckel, D. Weingarth and V. Presser, *Carbon*, **94**, 507 (2015);
https://doi.org/10.1016/j.carbon.2015.07.028

33. D. Lee, J. Seo, X. Zhu, J. Lee, H.-J. Shin, J.M. Cole, T. Shin, J. Lee, H. Lee and H. Su, *Sci. Rep.*, **3**, 2250 (2013);
https://doi.org/10.1038/srep02250

34. Y. Wang and A. Hu, *J. Mater. Chem. C Mater. Opt. Electron. Devices*, **2**, 6921 (2014);
https://doi.org/10.1039/C4TC00988F

35. R.N. Viswanath, D. Kramer and J. Weissmüller, *Langmuir*, **21**, 4604 (2005);
https://doi.org/10.1021/la0473759

36. R.N. Viswanath, D. Kramer and J. Weissmüller, *Electrochim. Acta*, **53**, 2757 (2008);
https://doi.org/10.1016/j.electacta.2007.10.049

37. M. Arenz, V. Stamenkovic, T.J. Schmidt, K. Wandelt, P.N. Ross and N.M. Markovic, *Surf. Sci.*, **523**, 199 (2003);
https://doi.org/10.1016/S0039-6028(02)02456-1

38. E. Wicke and H. Brodowsky, Eds., G. Alefeld and J. Völkel, Springer-Verlag, pp. 73-155 (1978).

39. S. Trasatti and O.A. Petrii, *Pure Appl. Chem.*, **63**, 711 (1991);
https://doi.org/10.1351/pac199163050711

40. N. Hoshi, K. Kagaya and Y. Hori, *J. Electroanal. Chem.*, **485**, 55 (2000);
https://doi.org/10.1016/S0022-0728(00)00098-X

41. Z. Radovic-Hrapovic and G. Jerkiewicz, *J. Electroanal. Chem.*, **499**, 61 (2001);
https://doi.org/10.1016/S0022-0728(00)00478-2

42. M. Hara, U. Linke and T. Wandlowski, *Electrochim. Acta*, **52**, 5733 (2007);
https://doi.org/10.1016/j.electacta.2006.11.048

43. A. Zalineeva, S. Baranton, C. Coutanceau and G. Jerkiewicz, *Sci. Adv.*, **3**, e1600542 (2017);
https://doi.org/10.1126/sciadv.1600542

44. V.S. Bagotsky, Fundamentals of Electrochemistry, Thermodynamics of Electrochemical System, Wiley Interscience, John Wiley & Sons Inc. Publications, New Jersey, Chap. 3 (2006);
https://doi.org/10.1002/047174199X